



Contents lists available at ScienceDirect

## Biochemical and Biophysical Research Communications

journal homepage: [www.elsevier.com/locate/ybbrc](http://www.elsevier.com/locate/ybbrc)

## The reduced trabecular bone mass of adult ARKO male mice results from the decreased osteogenic differentiation of bone marrow stroma cells

Meng-Yin Tsai<sup>a,b,1</sup>, Chih-Rong Shyr<sup>c,e,1</sup>, Hong-Yo Kang<sup>a,b</sup>, Yung-Chiao Chang<sup>a</sup>, Pei-Lin Weng<sup>a</sup>, Shu-Yo Wang<sup>a</sup>, Ko-En Huang<sup>a,\*</sup>, Chawnshang Chang<sup>d,e,f,\*</sup>

<sup>a</sup>Center for Menopause and Reproductive Medicine Research, Department of Obstetrics and Gynecology, Kaohsiung Chang-Gung Memorial Hospital, Kaohsiung, Taiwan

<sup>b</sup>Graduate Institute of Clinical Medical Science, Chang Gung University, Taoyuan, Taiwan

<sup>c</sup>Department of Medical Laboratory Science and Biotechnology, China Medical University, Taichung, Taiwan

<sup>d</sup>Graduate Institute of Clinical Medical Science, China Medical University, Taichung, Taiwan

<sup>e</sup>Sex Hormone Research Center, China Medical University Hospital, Taichung, Taiwan

<sup>f</sup>George H. Whipple Lab for Cancer Research, Departments of Pathology and Urology, University of Rochester Medical Center, Rochester, New York, USA

### ARTICLE INFO

#### Article history:

Received 2 June 2011

Available online 23 June 2011

#### Keywords:

Androgen receptor

Knock-out

Trabecular bone

Bone marrow stromal cells

Osteogenic differentiation

### ABSTRACT

Male mice with androgen receptor knock-out (ARKO) show significant bone loss at a young age. However, the lasting effect of AR inactivation on bone in aging male mice remains unclear. We designed this study to evaluate the effect of AR on bone quality in aging male mice and to find the possible causes of AR inactivation contributing to the bone loss. The mice were grouped according to their ages and AR status and their trabecular bones were examined by micro-CT analysis at 6, 12, 18, and 30 weeks old. We found that bone mass consistently decreased and the bone microarchitectures continuously deteriorated in male ARKO mice at designated time points. To determine the cause of the bone loss in ARKO mice, we further examined the role of AR in bone cell fate decision and differentiation and we conducted experiments on bone marrow stromal cells (BMSC) obtained from wild type (WT) and AR knockout (KO) mice. We found that ARKO mice had higher numbers of colony formation unit-fibroblast (CFU-F), and CD44 and CD34 positive cells in bone marrow than WT mice. Our Q-RT-PCR results showed lower expression of genes linked to osteogenesis in BMSCs isolated from ARKO mice. In conclusion, AR nullification disrupted bone microarchitecture and caused trabecular bone mass loss in male ARKO mice. And the fate of BMSCs was impacted by the loss of AR. Therefore, these findings suggest that AR may accelerate the use of progenitor cells and direct them into osteogenic differentiation to affect bone metabolism.

© 2011 Elsevier Inc. All rights reserved.

### 1. Introduction

Osteoporosis characterized by the loss of bone microarchitecture increases the risk of bone fractures. Men with either congenital or acquired hypogonadism suffer from osteoporosis [1–3]. Two clinical studies suggest that the combined use of estrogens and androgens might have synergistic effects in the prevention of osteoporosis in the elderly women, suggesting the protective role of androgen/androgen receptor (androgen/AR) signaling on bone [4,5]. However, the role of androgen/AR signaling in osteoporosis

is relatively unclear. Since bone fractures have become a heavy burden in global public health [6,7], studying the role of androgen/AR signaling is critical.

The bone metabolism involves two types of cells: osteoblasts derived from bone marrow mesenchymal cells for bone formation and osteoclasts derived from hematopoietic progenitor cells for bone resorption [8]. Androgens have been reported to affect osteoblast function by influencing the secretion of cytokines and growth factors [9]. AR was also shown to affect myogenic differentiation and adipogenic differentiation of mesenchymal pluripotent cells [10]. During rat calvarial osteoblasts differentiation, AR levels were lowest during proliferation, increased in the matrix maturation stage, and reached the highest levels in the most mature cultures, indicating that AR differentially modulated osteoblasts during the differentiation [11].

Previously, we studied the effects of AR on bone physiology using our own ARKO model. Our results showed significant bone loss in ARKO male mice [12]. A similar phenomenon has also been observed in other ARKO models [13]. The ARKO mice exhibit

\* Corresponding authors. Addresses: University of Rochester, School of Medicine and Dentistry, 601 Elmwood Ave, Box 626, Rochester, New York 14642, USA. Fax: +1 585 756 4133 (C. Chang), Center for Menopause and Reproductive Medicine Research, Chang Gung University and Chang Gung Memorial Hospital, 12F, No. 123, Ta Pei Rd., Niao Sung Hsiang, Kaohsiung 833, Taiwan. Fax: +886 7733 6970 (K.-E. Huang).

E-mail addresses: [khuang@adm.cgmh.org](mailto:khuang@adm.cgmh.org) (K.-E. Huang), [chang@urmc.rochester.edu](mailto:chang@urmc.rochester.edu) (C. Chang).

<sup>1</sup> These authors contributed equally to the article.

abnormal number and size of adipocytes [12] and late onset obesity in male ARKO mice because of increased adipocytes [13]. These results showing the disrupted adipogenesis and osteogenesis due to the loss of AR suggest that AR affects the process of osteoblastic and adipocytic differentiation, which could take place in bone marrow stroma cells (BMSCs) to affect bone metabolism. BMSCs are able to self-renew to produce daughter cells, but can also differentiate into a variety of cell types [14,15]. Because of the capability of BMSCs to turn into multiple mesenchymal cell lineages such as osteoblasts, chondrocytes, and adipocytes, these cells are also referred to as mesenchymal stem cells [16,17]. BMSCs were found to exist in colony-forming units-fibroblasts (CFU-F) detected in the bone marrow by using *in vitro* colony assay [18].

To determine the role of AR in bone metabolism throughout the lifespan and whether it involves BMSCs, we compared the microarchitecture of trabecular bones of ARKO and WT mouse femurs and isolated BMSCs from the bone marrow of both WT and ARKO mice. Our results demonstrated that the loss of AR caused the deterioration of bone structures and the BMSCs to change their intrinsic self-renewal/differentiation potential. In summary, the loss of AR caused the increased progenitor cell numbers with less cells differentiating to bone cells, resulting in consistent bone loss. Therefore, AR acts in favoring the progenitor cell differentiation decision for osteogenesis. This study could help us understand the pathophysiological role and cellular mechanisms of androgen/AR signaling on bone metabolism.

## 2. Materials and methods

### 2.1. Animals

The detailed procedures for the generation of floxAR mice and genotyping confirmation have been described in our previous paper [12]. All study mice had a C57BL/6-129/SEVE background. All animal procedures followed the Guide for the Care and Use of Laboratory Animal of the Institute of Laboratory Animal Resources, National Research Council, National Academy of Sciences, USA and were approved by the animal care and use committee of the Chang Gung Memorial Hospital, Kaohsiung. Construction of targeting vectors and generation of chimera founder mice and subsequent ARKO mice have been described previously [12]. Animals were housed in specific pathogen-free facilities and maintained on a 12-h light/dark schedule (light on at 0600).

### 2.2. Micro-CT analysis

Micro-CT analysis was done on the right femur using a Skyscan 1076 scanner (Skyscan, Belgium). The mice were offsprings of mice we previously studied [12]. We scanned the right femur of the mice. The scanning images were developed using an X-ray tube voltage of 45 kV and current 100  $\mu$ A, with a 0.5 mm aluminum filter. The image slices were reconstructed using the NRecon (v.1.4.4; Skyscan) software system. The 3-dimensional parameters of bone microarchitecture were calculated using CTAn (v.1.7.0.0; Skyscan) software. For trabecular bone, the distal femur was selected for analysis within a conforming volume of interest commencing at the growth plate and extending a further longitudinal distance of 0.9 mm in the proximal direction. A total of 100 image slices were analyzed for each femur. The parameters measured included the percentage of bone volume versus total volume (BV/TV%), trabecular thickness (Tb. Th), trabecular number (Tb. N), and trabecular separation (Tb. Sp).

### 2.3. Cell culture

The bone marrow cells ( $5 \times 10^5$  cells/well) flushed from femurs of 8–12 week old WT or ARKO mice were cultured in 35 mm collagen type I coated dish (Falcon) with  $\alpha$ MEM containing 15% FBS (Invitrogen), 100 U/mL penicillin/streptomycin (Invitrogen), 2 mM L-glutamine (Invitrogen), and 10 mM  $\beta$ -glycerol phosphate (Sigma) for 48 h. After washing out non-adherent haematopoietic cells, total stromal cells were cultured for 14 days in 5% CO<sub>2</sub> at 37 °C. The cells were fixed with 100% methanol for 10 min at –20 °C and stained with 0.1% methylene blue (Riedel-deHaën) for 10 min at RT. The colonies showing more than 50 aggregate cells were counted as colony-forming units-Fibroblasts (CFU-Fs).

For osteogenic differentiation, we treated cells with 10 mM  $\beta$ -glycerol phosphate (Sigma),  $1 \times 10^{-6}$  M dexamethasone (TOCRIS) and 50  $\mu$ g/mL ascorbate 2-phosphate (sigma) cultured for 5, 10, and 15 days in 5% CO<sub>2</sub> at 37 °C. The cells were then collected for RNA extraction for real-time quantitative RT-PCR experiments.

### 2.4. Immuno-cytochemical staining and Western blotting

The cells were fixed in 100% methanol in –20 °C and blocked with blocking solution with 10% FBS in PBS and incubated at room temperature for 1 h, and then incubated with a 1:100 dilution of primary antibody (Anti-AR antibodies, Santa Cruz Biotechnology, Inc.) overnight at 4 °C. We then incubated the samples with a 1:200 dilution of peroxidase-conjugated anti-rabbit IgG (Vector Laboratories, Burlingame, CA). The cells were washed with PBS for further color development by using 3,3'-diaminobenzidine tetra-hydrochloride as chromogenic substrate for conjugated peroxidases (K3468, liquid DAB+ kit; Dako). Cells were then counterstained with hematoxylin.

### 2.5. FACS analysis

The antibodies CD44-FITC (fluorescein isothiocyanate) and CD34-PE (phycoerythrin) were obtained from eBioscience. BMSCs cultured in  $\alpha$ MEM were released with trypsin/EDTA and counted. About  $5 \times 10^5$  cells were divided into aliquots in amber-tinted 1.5-mL centrifuge tubes and pelleted by centrifugation for 5 min at 2000 rpm. The cells were resuspended in 0.2 mL PBS. FITC-conjugated antibodies were added at a concentration of 0.5  $\mu$ g, and PE-conjugated antibodies at 1  $\mu$ g. The samples were incubated at 4 °C for 40 min in the dark. The cells were pelleted, washed twice with PBS, and analyzed by flow cytometry.

### 2.6. RNA isolation and real-time quantitative RT-PCR

TRIzol reagent (Invitrogen, Carlsbad, CA) was used to extract total RNA from the cells following the manufacturer's instructions. After checking the RNA quality by spectrophotometer, 2  $\mu$ g of RNA was used for cDNA synthesis using the ThermoScript first strand cDNA synthesis reverse transcription-PCR System (Promega, USA) with procedures suggested by the manufacturer.

Real time quantitative RT-PCR was performed for bone markers, including *Runx2/Cbfa1*, collagen 1a1 (*Col1a1*), and osteocalcin (*Ocn*) for osteoblast formation. The sequences of the primers for AR,  $\beta$ -actin, *Col1a1*, *Runx2/Cbfa1*, and *Ocn* were used as described in our previous paper [19]. The reactions were carried out in an Applied Biosystems 7700 system using Power SYBR Green PCR Master Mix (Applied Biosystems). The sequential reaction conditions for all markers were 95 °C for 10 min, followed by 40 cycles of 95 °C for 20 s, 60 °C for 30 s and 72 °C for 30 s. Gene expression was quantified using the sequence detection software of the system (Applied Biosystems).  $\beta$ -actin was used as the housekeeping gene for data normalization. Data were obtained from at least

three separate experiments. Every marker gene was assayed in triplicate for each experiment.

### 2.7. Statistical analysis

All data were analyzed by the independent-samples *t* test. For all statistical analyses, a value of  $p < 0.05$  was considered significant. Data are presented as means  $\pm$  SD.

## 3. Results and discussion

### 3.1. The osteoporotic phenotypes of young androgen receptor knockout (ARKO) mice

AR has been demonstrated to link to the development and maintenance of bones. So to further examine the role of AR in the microarchitectures of trabecular bones as mice aged, we used micro-CT scanner to obtain 3D images of trabecular bones and measured the bone histomorphometric parameters of the distal metaphysis of the femur. First, 6 weeks old WT and ARKO male

mice were analyzed. The results are displayed in Fig. 1A–E. ARKO mice showed a reduction in trabecular bone volume ( $-17\%$ ) (Fig. 1B) and number ( $-12\%$ ) (Fig. 1D), but the similar thickness of trabecular bone, when compared to WT control mice (Fig. 1C). Furthermore, the male ARKO mice had significantly wider trabecular separation ( $20\%$ ) than male WT mice (Fig. 1E). At 12 weeks of age, micro-CT analyses also showed significant differences in the trabecular bone composition between the 12 weeks old WT and ARKO male mice (Fig. 1A–E, right panels). The bones in the WT mice were more compact and had more trabeculae than those in the ARKO mice. The percentage of bone volume (BV) versus total volume (TV) (BV/TV%) was significantly lower in ARKO mice ( $-32\%$ ) (Fig. 1B). The decrease was due to a decreased number ( $-34\%$ ) of trabeculae (Fig. 1D) and increased distance between intertrabeculae ( $+85\%$ ) (Fig. 1E) in the ARKO mice. These data indicate that AR plays a role in bone microstructure and this effect is greater in males at 12 weeks old than 6 weeks old. And the decreased BV/TV% in ARKO mice was because of decreased trabecular number and increased trabecular separation, because the trabecular thickness was similar between the WT and ARKO mice.

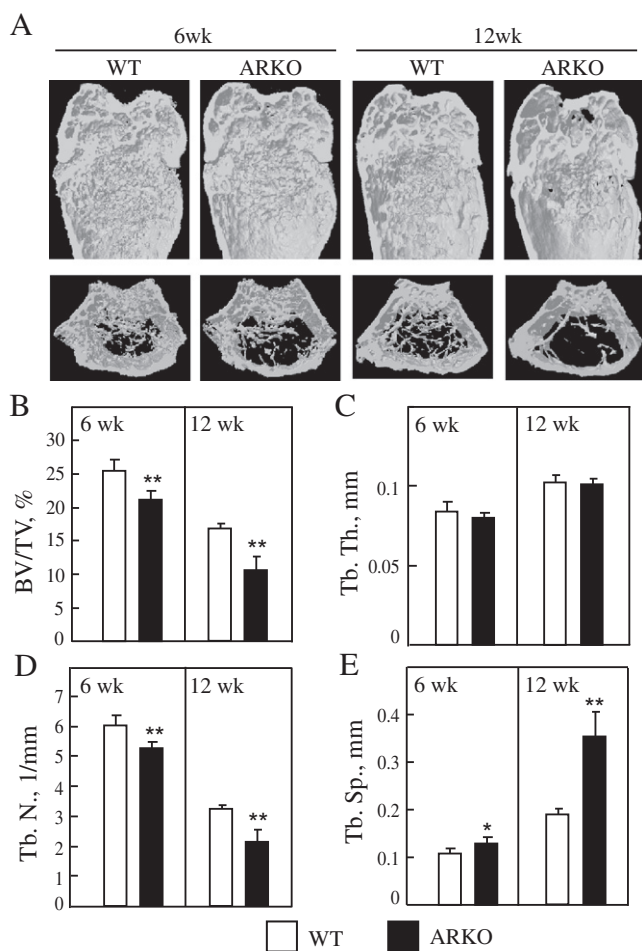


**Fig. 1.** Micro-CT images and computer-aided analysis of the trabecular femoral bones of 6 and 12 week-old mice. ARKO and WT male mice at 6 and 12 weeks old were used for imaging studies, evaluating trabecular bone in the metaphysis of the distal femur. (A) Representative 3D  $\mu$ CT images of trabecular bone in the distal femurs of 6 and 12 weeks old mice, (B) percent bone volume (BV/TV%), (C) trabecular thickness (Tb. Th., mm), (D) trabecular number (Tb. N., 1/mm), and (E) trabecular separation (Tb. Sp., mm) in male and female WT and ARKO mice at 6 and 12 weeks old. Values are given as means  $\pm$  SD. \* $p < 0.05$ , \*\* $p < 0.01$ ; significantly different between WT and ARKO ( $n = 4-5$ ) mice as assessed by independent-samples *t*-test.

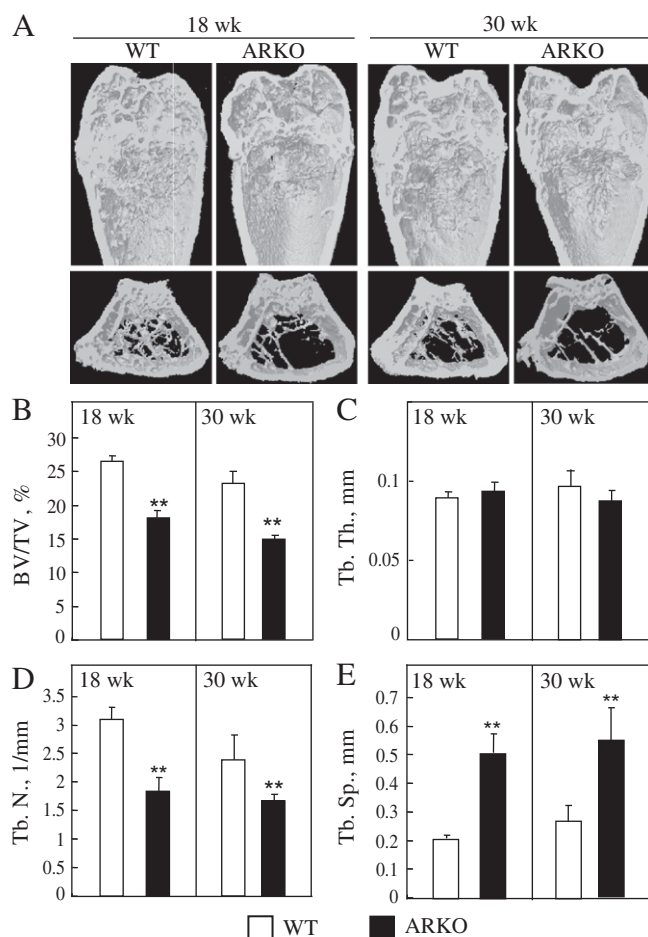


**Fig. 2.** Micro-CT images and computer-aided analysis of the trabecular femoral bones of 18 and 30 weeks old mice. ARKO and WT male mice at 18 and 30 weeks old were used for imaging studies, evaluating trabecular bone in the metaphysis of the distal femur. (A) Representative 3D  $\mu$ CT images, (B) percent bone volume (BV/TV%), (C) trabecular thickness (Tb. Th., mm), (D) trabecular number (Tb. N., 1/mm), and (E) trabecular separation (Tb. Sp., mm). Values are given as means  $\pm$  SD. \* $p < 0.05$ , \*\* $p < 0.01$ ; significantly different between WT and ARKO ( $n = 4-5$ ) mice as assessed by independent-samples *t*-test.

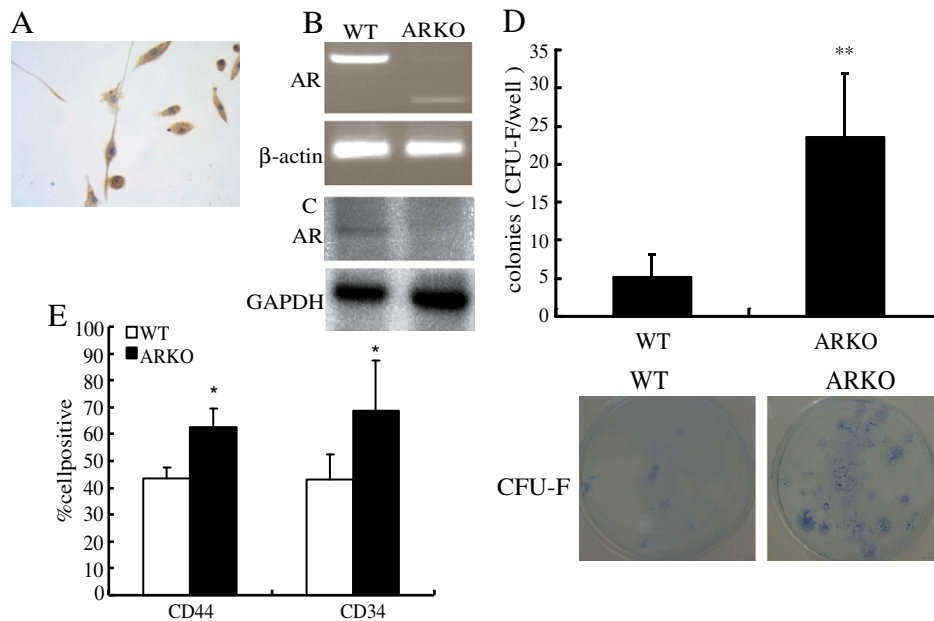


**Fig. 3.** The change of cell population in BMSCs from ARKO mice. The expression of AR on BMSC was demonstrated by Immunostaining, RT-PCR and Western blotting. (A) Immuno-cytochemical staining of ARKO BMSC with anti-AR (C19) antibody, as indicated. (B) Expression of AR in WT and ARKO BMSCs was detected after 3 weeks of culture by RT-PCR of total RNA extract from parallel culture with  $\beta$ -actin as an internal control for RNA abundance. (C) Immunoblot of protein extract from WT and ARKO BMSC with anti-AR (C19) and GAPDH was blotted for protein loading control. (D) The CFU-F assay of bone marrow cells isolated from ARKO and WT mice. (E) The comparison of cell epitopes between WT and ARKO by FACS. Primary cultured BMSCs from WT and ARKO were stained with antibodies for CD44-FITC, and CD34-PE and determined by FACS. Data are presented as means  $\pm$  SD ( $n = 3$ –8 individual mice). \* $p < 0.05$ , \*\* $p < 0.01$ ; significantly different from WT control as assessed by independent-samples  $t$ -test.

### 3.2. The osteoporotic phenotypes of adult and aging androgen receptor knockout (ARKO) mice

To observe the continuous effects of ARKO on bone, we examined the adult 18 weeks old and aged 30 weeks old mice. We also compared the trabecular bones from ARKO or WT mice. The results of micro-CT analysis of 18 week-old mice are displayed in Fig. 2A–E and the three dimensional (3D) micro-CT pictures clearly displayed that the bone mass was significantly decreased in male ARKO. The ARKO mice had lower bone volume (–34%) (Fig. 3B), fewer trabeculae (–41%) (Fig. 2D), but wider separations (143%) (Fig. 2E) than WT mice. At age of 30 weeks (Fig. 2A–E), ARKO mice showed a reduction in trabecular bone volume (–30%) (Fig. 2B) and number (–36%) (Fig. 2D), but similar thickness of trabecular bone, when compared to WT control mice (Fig. 2C). Furthermore, the male ARKO mice had significantly wider trabecular separation (102%) than male WT mice (Fig. 2E). Therefore the decrease of bone mass was mainly due to the decreased numbers of trabeculae and increased trabecular separation (Figs. 1 and 2), indicating the bone failed to rebuild after loss due to high bone turnover. Previous studies only reported the trabecular bone loss of global ARKO mice up to 8 weeks old mice. Whether the bone loss of ARKO mice could be recovered after maturation was not further examined [12,13,20].

Therefore in this study, we examined the effect of the loss of AR on trabecular bone in up to 30 weeks old mice and observed that the osteoporotic phenotypes were consistently found in ARKO mice (Fig. 2A–E). The osteoblast-specific ARKO mice with second zinc finger-deficient AR showed that femur trabecular bone volume (–24%) and numbers (–3%) were reduced at 30 weeks of age, but not overtly different at 6 and 12 weeks old compared to control mice [21]. The trabecular bone changes of osteoblast-specific ARKO mice were less than those of global ARKO mice of 30 weeks old reported in the present study, indicating that osteoblasts are not the sole AR target cells to affect bone development and metabolism. In addition to the proposed suppressive function

of AR in osteoblasts to repress osteoclastogenesis by down-regulating the expression of the receptor activator of NF-kappaB ligand (Rankl) gene, which encodes a major osteoclastogenesis inducer [13], our results indicate another possible role of AR in increasing progenitor cell differentiation into bone cells to affect bone metabolism.

### 3.3. AR affects the number of progenitor cells in bone marrow stromal cells

We found that ARKO mice had trabecular bone loss and deteriorated bone microarchitecture throughout the lifespan and the destructive effect of AR loss on bone was peaked at 18 weeks old, suggesting a lasting effect of AR loss. To study the role of AR in osteogenesis and answer the possible causes of the osteopenic phenotypes in ARKO mice, we further investigated the action of AR on the osteogenic differentiation of BMSCs. To prove that AR plays a role in BMSCs, we first examined the expression of AR on BMSCs isolated by their ability to adhere on plastic tissue culture plates. Using immunostaining methods, we saw the expression of AR in BMSCs (Fig. 3A). RT-PCR and Western blotting experiments also demonstrated the presence of AR protein and RNA in BMSCs, but for ARKO BMSCs, we observed the absence of the AR (Fig. 3B–C). And we further determined the effect of the loss of AR on the progenitor cell number of BMSCs. To investigate whether AR loss affects the progenitor number in BMSCs, we used colony formation unit assay to measure the number of these progenitor cells. The CFU-F is formed when marrow cells are cultured *in vitro* as a cluster of cells, which has a high ability for self-renewal and multipotentiality [16]. After isolating bone marrow cells from 8 to 12-week-old WT or ARKO mice, equal numbers of nucleated bone marrow cells were cultured. The number of CFU-Fs, a measurement of total mesenchymal precursors including stem cells and committed progenitors, formed in ARKO compared with WT cultures was increased by 4 folds (Fig. 3D). To determine whether the proportion of cell population in BMSC culture will be changed

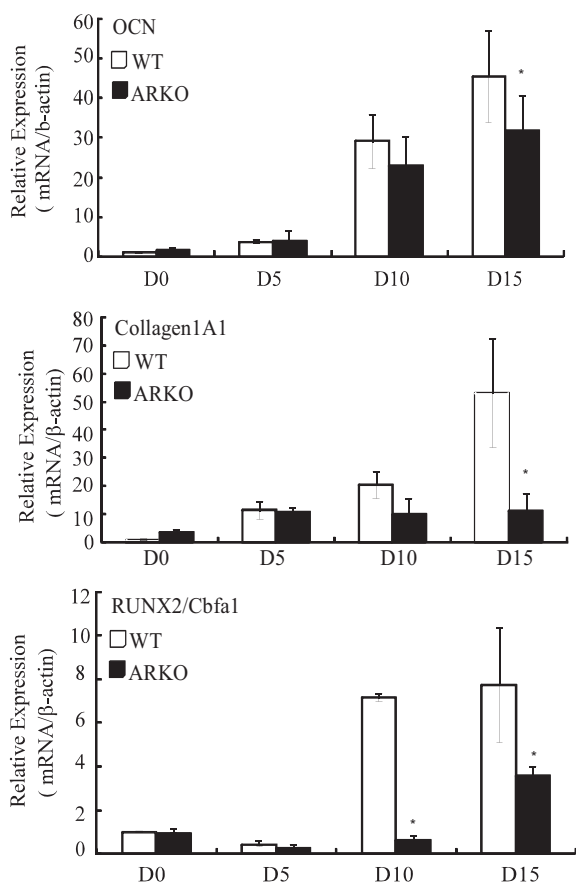


**Fig. 4.** The effect of AR on the osteogenesis-related marker gene expression during BMSC differentiation into osteoblastic lineage. BMSCs from ARKO and WT mice were induced into osteoblastic differentiation. The RNAs were collected at different days after induced differentiation and examined by qRT-PCR. Data are presented as means  $\pm$  SD ( $n = 4-6$  individual mice). \* $p < 0.05$ ; significantly different from WT controls as assessed by independent-samples  $t$ -test.

due to the loss of AR, we used monoclonal antibodies against several cell surface markers to characterize the cell population by flow cytometry. WT primary cultured marrow stromal cells were stained 43.4% for CD44 positive cells and 43.2% for CD34 positive cells. But cells from ARKO primary marrow stromal cell culture were stained 62.7% for CD44 positive cells and 68.7% for CD34 positive cells (Fig. 3E). These data demonstrate that mesenchymal progenitors (potential stem cells) were increased in ARKO BMSCs compared with those in WT mice. Therefore, we inferred that androgen/AR signaling could consistently affect the bone metabolism from development to maintenance by regulating BMSCs, the progenitor cells of osteoblasts, with ability to affect their self-renewal and differentiation ability. Although AR is expressed in osteoblasts and affects their growth and differentiation [19,22], here we further reported that the progenitor cells of osteoblasts in BMSCs are also the targets of androgen/AR signaling.

#### 3.4. The effects of AR on BMSC differentiation into osteoblastic or adipogenic lineage

To examine the molecular mechanism by which AR exerts to affect the osteogenic differentiation of BMSCs, we measured the osteogenesis-related marker genes (*Ocn*, *Col1a1* and *Runx2/Cbfa1*) at different time points when BMSCs were induced to differentiate into osteoblasts. The results (Fig. 4) showed that the expression of different marker genes increased as cells were induced into osteogenic lineage cells in WT BMSCs. But for ARKO BMSCs, the

expression of different marker genes was lower than that of WT BMSCs. These results suggest that ARKO BMSCs remain in more primitive state. The loss of AR caused the decrease of driving potential to differentiation. AR has the capacity to promote cell differentiation because previous studies have linked AR role in cell differentiation, such as myocyte, osteoblast, and adipocyte differentiation [10,11,23], indicating that AR is a critical factor in deciding the cell fates for the progenitor cells in response to the differentiating stimuli to the cells. Therefore, the loss of AR caused life-long osteoporosis since the defect in mesenchymal stem or progenitor cells was linked to age-dependent osteoporosis [24].

#### 4. Conflict of interest

The authors have no conflict of interest to disclose with regard to the subject matter of the present manuscript.

#### Acknowledgments

This study was supported by Grant CMRPG83047 and CMRPG830473 from Chang Gung Memorial Hospital, Taiwan, and NSC 94-2314-B-182A-143- and NSC 96-2321-B-320-002- from National Science Council, Taiwan. This study was also supported in part by Taiwan Department of Health Clinical Trial and Research Center of Excellence (DOH100-TD-B-111-004).

#### References

- [1] D.A. Smith, M.S. Walker, Changes in plasma steroids and bone density in Klinefelter's syndrome, *Calcif. Tissue Res.* 22 (Suppl) (1977) 225–228.
- [2] C. Foresta, G. Ruzza, R. Mioni, A. Meneghello, C. Baccichetti, Testosterone and bone loss in Klinefelter syndrome, *Horm. Metab. Res.* 15 (1983) 56–57.
- [3] H.W. Daniell, Osteoporosis due to androgen deprivation therapy in men with prostate cancer, *Urology* 58 (2001) 101–107.
- [4] N.B. Watts, M. Notelovitz, M.C. Timmons, W.A. Addison, B. Wiita, L.J. Downey, Comparison of oral estrogens and estrogens plus androgen on bone mineral density, menopausal symptoms, and lipid-lipoprotein profiles in surgical menopause, *Obstet. Gynecol.* 85 (1995) 529–537.
- [5] L.G. Raisz, B. Wiita, A. Artis, A. Bowen, S. Schwartz, M. Trahiotis, K. Shoukri, J. Smith, Comparison of the effects of estrogen alone and estrogen plus androgen on biochemical markers of bone formation and resorption in postmenopausal women, *J. Clin. Endocrinol. Metab.* 81 (1996) 37–43.
- [6] R. Burge, B. Dawson-Hughes, D.H. Solomon, J.B. Wong, A. King, A. Tosteson, Incidence and economic burden of osteoporosis-related fractures in the United States 2005–2025, *J. Bone Miner. Res.* 22 (2007) 465–475.
- [7] O. Johnell, J.A. Kanis, An estimate of the worldwide prevalence and disability associated with osteoporotic fractures, *Osteoporos Int.* 17 (2006) 1726–1733.
- [8] D. Vanderschueren, L. Vandenput, S. Boonen, M.K. Lindberg, R. Bouillon, C. Ohlsson, Androgens and bone, *Endocr. Rev.* 25 (2004) 389–425.
- [9] S.C. Manolagas, S. Kousteni, R.L. Jilka, Sex steroids and bone, *Recent Prog. Horm. Res.* 57 (2002) 385–409.
- [10] R. Singh, J.N. Artaza, W.E. Taylor, N.F. Gonzalez-Cadavid, S. Bhasin, Androgens stimulate myogenic differentiation and inhibit adipogenesis in C3H 10T1/2 pluripotent cells through an androgen receptor-mediated pathway, *Endocrinology* 144 (2003) 5081–5088.
- [11] K.M. Wiren, A. Chapman Evans, X.W. Zhang, Osteoblast differentiation influences androgen and estrogen receptor- $\alpha$  and - $\beta$  expression, *J. Endocrinol.* 175 (2002) 683–694.
- [12] S. Yeh, M. Tsai, Q. Xu, X. Mu, H. Lardy, K. Huang, H. Lin, S. Yeh, S. Altuwajiri, X. Zhou, Generation and characterization of androgen receptor knockout (ARKO) mice: an in vivo model for the study of androgen functions in selective tissues, *Proc. Natl. Acad. Sci. USA* 99 (2002) 13498.
- [13] H. Kawano, T. Sato, T. Yamada, T. Matsumoto, K. Sekine, T. Watanabe, T. Nakamura, T. Fukuda, K. Yoshimura, T. Yoshizawa, K. Aihara, Y. Yamamoto, Y. Nakamichi, D. Metzger, P. Chambon, K. Nakamura, H. Kawaguchi, S. Kato, Suppressive function of androgen receptor in bone resorption, *Proc. Natl. Acad. Sci. USA* 100 (2003) 9416–9421.
- [14] M.F. Pittenger, A.M. Mackay, S.C. Beck, R.K. Jaiswal, R. Douglas, J.D. Mosca, M.A. Moorman, D.W. Simonetti, S. Craig, D.R. Marshak, Multilineage potential of adult human mesenchymal stem cells, *Science* 284 (1999) 143–147.
- [15] D.J. Prockop, Marrow stromal cells as stem cells for nonhematopoietic tissues, *Science* 276 (1997) 71–74.
- [16] M. Owen, Marrow stromal stem cells, *J. Cell Sci. Suppl.* 10 (1988) 63–76.
- [17] Y. Jiang, B.N. Jahagirdar, R.L. Reinhardt, R.E. Schwartz, C.D. Keene, X.R. Ortiz-Gonzalez, M. Reyes, T. Lenvik, T. Lund, M. Blackstad, J. Du, S. Aldrich, A. Lisberg, W.C. Low, D.A. Largaespada, C.M. Verfaillie, Pluripotency of mesenchymal stem cells derived from adult marrow, *Nature* 418 (2002) 41–49.

- [18] A.J. Friedenstein, J.F. Gorskaja, N.N. Kulagina, Fibroblast precursors in normal and irradiated mouse hematopoietic organs, *Exp. Hematol.* 4 (1976) 267–274.
- [19] H.Y. Kang, C.L. Cho, K.L. Huang, J.C. Wang, Y.C. Hu, H.K. Lin, C. Chang, K.E. Huang, Nongenomic androgen activation of phosphatidylinositol 3-kinase/Akt signaling pathway in MC3T3-E1 osteoblasts, *J. Bone Miner. Res.* 19 (2004) 1181–1190.
- [20] K. Venken, K. De Gendt, S. Boonen, J. Ophoff, R. Bouillon, J.V. Swinnen, G. Verhoeven, D. Vanderschueren, Relative impact of androgen and estrogen receptor activation in the effects of androgens on trabecular and cortical bone in growing male mice: a study in the androgen receptor knockout mouse model, *J. Bone Miner. Res.* 21 (2006) 576–585.
- [21] A.J. Notini, J.F. McManus, A. Moore, M. Bouxsein, M. Jimenez, W.S. Chiu, V. Glatt, B.E. Cream, D.J. Handelsman, H.A. Morris, J.D. Zajac, R.A. Davey, Osteoblast deletion of exon 3 of the androgen receptor gene results in trabecular bone loss in adult male mice, *J. Bone Miner. Res.* 22 (2007) 347–356.
- [22] C.H. Kasperk, K. Faehling, I. Borcsok, R. Ziegler, Effects of androgens on subpopulations of the human osteosarcoma cell line SaOS2, *Calcif. Tissue Int.* 58 (1996) 376–382.
- [23] S. Altuwajiri, D.K. Lee, K.H. Chuang, H.J. Ting, Z. Yang, Q. Xu, M.Y. Tsai, S. Yeh, L.A. Hanchett, H.C. Chang, C. Chang, Androgen receptor regulates expression of skeletal muscle-specific proteins and muscle cell types, *Endocrine* 25 (2004) 27–32.
- [24] M. Bonyadi, S.D. Waldman, D. Liu, J.E. Aubin, M.D. Grynopas, W.L. Stanford, Mesenchymal progenitor self-renewal deficiency leads to age-dependent osteoporosis in Sca-1/Ly-6A null mice, *Proc. Natl. Acad. Sci. USA* 100 (2003) 5840–5845.